

# ON THE RESPONSE OF THE CAR FROM ROAD DISTURBANCES

RĂZVAN-VLAD VASIU<sup>1</sup>, OCTAVIAN MELINTE<sup>2</sup>, VICTOR VLĂDĂREANU<sup>2</sup>, DAN DUMITRIU<sup>2</sup>

*Abstract.* The tire/road contact dynamics is investigated in this paper by assuming a rocky road. The vehicle model to be used in simulation is a seven degree of freedom full-car model. The contact domain between the tire and the road has a shape defined by the Lamé curve, and it is identified by checking the minimum distance between bodies in contact. The nonlinear response from road disturbances is analyzed by assuming explicit relationships for contact and friction forces, respectively. Since the road is rocky, a bristle model was chosen to take into account the effect of the road irregularities on the tire's action.

*Key words:* full-car vehicle model, contact force, friction force, rocky road, contact dynamics.

## 1. INTRODUCTION

The impact and the frictional slip are met together when they simultaneously develop in a contact interface, such as the interface between the tire and the road. The distribution of forces can be manifested in many different forms and the friction model changes the characteristics of the vibro-impact phenomenon in terms of duration, dissipation of energy, accelerations and decelerations [1–4].

The irregularities of the road (bumps, corners, peaks, shallows, etc.) can not be taken into account without introducing the contact and friction forces in the contact interfaces. We adopt in this paper a continuum approach for the vibro-contact dynamics by admitting explicit relationship between contact force and deformation. In this continuous approach, no difference is made between impact and contact, therefore the methods of non-impact dynamics can be used to solve the problem [4]. The modeling of the contact friction in the interfaces has been performed in a series of relevant papers [5–10]. The contact force depends on the deformation and it is defined by the interference distance or penetration. Impacts between bodies are generally defined by the condition of impenetrability [11].

The continuum modeling of tire/road vibro-contact dynamics is developed in this paper for a rocky road and the contact domain is modeled by checking the minimum distance between bodies. The model takes as inputs the function of

---

<sup>1</sup> Technical University of Cluj-Napoca, Faculty of Mechanics, Cluj-Napoca, Romania

<sup>2</sup> Institute of Solid Mechanics of the Romanian Academy, Bucharest, Romania

bristle displacement and the vertical tire force and produces, as outputs, the distribution of contact pressure in the interfaces between the tire and the road in a short interval of time.

The novelty of the paper in relation to mentioned publications from the literature is referring to the modeling of the tire/road contact for a rocky road. Modelings for such roads we do not found in the literature. For such roads only the bristle model is able to take into account the effect of the irregularities on the tire's action. Our modeling is based on a seven degree of freedom full-car model. The idea of taking the Lamé curve for modeling the contact domain between the tire and the road is new. This idea together with the explicit relationships for contact and friction forces in the contact interfaces, form a new strategy introduced in this paper for investigation the tire behavior on rocky roads.

## 2. CONTACT BETWEEN THE TIRE AND THE ROAD

The contact between the tire and the road can be identified by checking the minimum distance between the tire and the road [5]

$$\min\left(\frac{1}{2}(r_1 - r_2)^T(r_1 - r_2)\right), \quad f_1(r_1) \leq 0, \quad f_2(r_2) \leq 0, \quad (1)$$

where  $r_1$  and  $r_2$  are the position vectors of two points belonging to the tire and the road, respectively, and  $f_1$  and  $f_2$  are bounding surface constraints. The interference distance is defined as

$$\min(-d), \quad f_1(r_1) \leq -\frac{d}{2}e_1, \quad f_2(r_2) \leq -\frac{d}{2}e_2. \quad (2)$$

The tire load and velocity generate forces at the interface between the tire and the road. These forces act in three directions, namely the contact force  $F_c = F_{cz}$  acting in the  $z$  direction, the longitudinal component of the friction force  $F_{tx}$  acting in the  $x$  direction, and the lateral component of the friction force  $F_{ty}$  acting in the  $y$  direction, respectively (Fig. 1).

Figure 2 shows the force and moments vectors acting on an arbitrary point  $P$  of the tire located at the central intersection point of the tire and road surface plane. The undeformed tire has the radius  $R$  and rotates at constant angular speed  $\Omega$  about the wheel axis. In the tire plane  $x$  and  $y$  axes are parallel to the longitudinal axis of the tire and the road surface normal, respectively.  $F_x$  is the longitudinal force acting in the direction of the forward motion of the tire in the plane of the road,  $F_y$  is the lateral force acting in the direction perpendicular to  $F_x$  in the plane of the road, and  $F_z$  is the vertical force acting in the direction of the vector normal to the road plane.  $M_x$  is the overturning moment acting about the axis parallel to  $F_x$  vector,  $M_y$  is the

rolling resistance moment acting about the axis parallel to the  $F_y$  vector, and  $M_z$  is the aligning moment acting about the axis parallel to  $F_z$  vector.

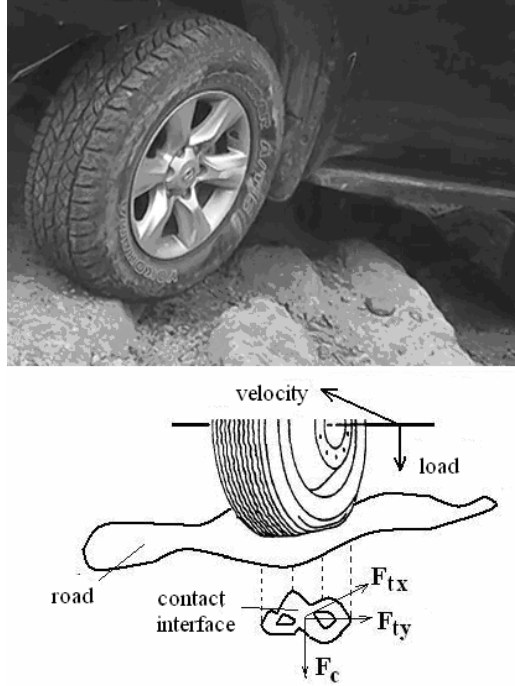


Fig. 1 – The contact between the tire and the road.

The  $\tau$ ,  $|\tau| < 90^\circ$  is the slip angle between the travel direction and the direction in which the tire is oriented,  $\gamma$  is the camber angle, that means the inclination angle between the  $z$ -axis and the tire plane and  $\omega$  is the angular velocity of the wheel measured at the centre of the wheel-tire assembly (the linear speed of the center of the wheel in the longitudinal direction is  $V$ ), and  $T$  is the axle torque.

If we denote with  $p_x$ ,  $p_y$  and  $p_z$ , the longitudinal tire contact stress, the lateral tire contact stress and vertical tire contact pressure, the forces and moments, respectively in the point  $P(x, y)$  belonging to the contact area  $A$  are given by

$$F_x(P) = -\int_A p_x dA, \quad F_y(P) = -\int_A p_y dA, \quad F_z(P) = -\int_A p_z dA, \quad (3)$$

$$M_x(P) = -\int_A p_z \cdot y dA, \quad M_y(P) = \int_A p_z \cdot x dA, \quad M_z(P) = \int_A (p_x \cdot y - p_y \cdot x) dA. \quad (4)$$

From (1.3) and (1.4) we can determine the forces  $F_x, F_y, F_z$  and moments  $M_x, M_y, M_z$  acting at the center of the tire in the tire reference frame, by applying a rotation  $\gamma$  about  $x$  [12]

$$\begin{pmatrix} F_x(P) \\ F_y(P) \\ F_z(P) \end{pmatrix} = \begin{pmatrix} 1 & 0 & 0 \\ 0 & \cos \gamma & -\sin \gamma \\ 0 & \sin \gamma & \cos \gamma \end{pmatrix} \begin{pmatrix} F_x \\ F_y \\ F_z \end{pmatrix},$$

$$\begin{pmatrix} 1 & 0 & 0 \\ 0 & \cos \gamma & -\sin \gamma \\ 0 & \sin \gamma & \cos \gamma \end{pmatrix} \begin{pmatrix} M_x \\ M_y \\ M_z \end{pmatrix} = \begin{pmatrix} M_x(P) - F_y(P)R \cos \gamma - F_z(P)R \sin \gamma \\ M_y(P) + F_x(P)R \cos \gamma \\ M_z(P) + F_x(P)R \sin \gamma \end{pmatrix}. \quad (5)$$

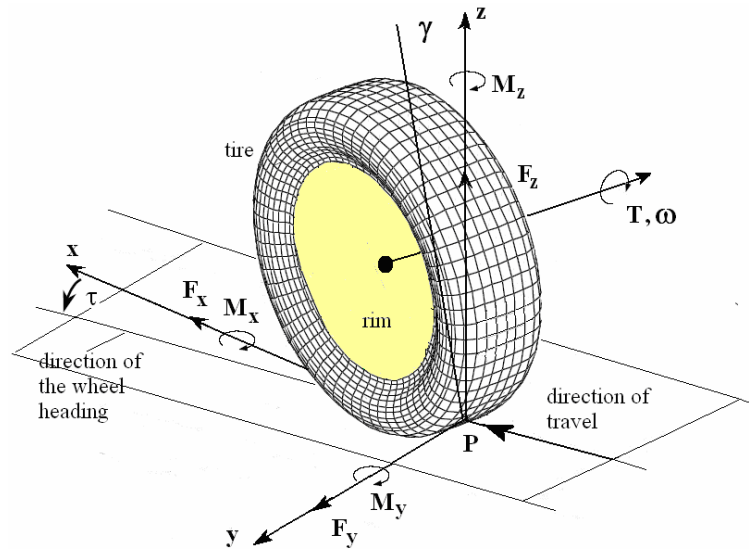


Fig. 2 – Forces and moments acting on the tire.

To shape of the unknown contact domain between the tire and the road is taken as a superellipse shape defined by the Lamé curve [8],[9]

$$\left(\frac{x}{a(t)}\right)^n + \left(\frac{y}{b(t)}\right)^n = 1, \quad n > 0, \quad (6)$$

where  $x$  and  $y$  define the envelope of the contact area,  $a$  is half of the contact length,  $b$  is half of the contact width (radii of the oval shape are depending of time), and  $n$  the power of the ellipsoid.

For the contact area  $A$  area of (6), we have

$$A(t) = 4b \int_0^a \left(1 - \left(\frac{x}{a}\right)^n\right)^{1/n} dx = \frac{4^{1-1/n} a(t)b(t)\sqrt{\pi}\Gamma\left(1 + \frac{1}{n}\right)}{\Gamma\left(\frac{1}{2} + \frac{1}{n}\right)}, \quad (7)$$

where  $\Gamma$  is the Gamma function

$$\Gamma(z) = \lim_{n \rightarrow \infty} \frac{n!n^z}{z(z+1)\dots(z+n)} \quad (z \neq 0, -1, -2, \dots).$$

### 3. MODEL DESCRIPTION

The description of the car is carried out based on the papers [13–15]. An alternative approach can be found in [16] concerning only the vertical dynamics by using a 7 DOF car model. The dynamic contact between the wheels and the road cannot be studied by alone, but only considering the car as a unique dynamical system. The sprung mass  $m$  of the vehicle is defined as a rigid body that can translate and rotate, exhibiting angular oscillations around the mass centre  $G$ . The tires  $B_j$ ,  $j=1,2,3,4$  are represented as the tips of the tetrahedron  $Q$ . The trajectories of these tips are arbitrary in the space, but subjected to given geometric requirements. Let us consider in the following that the projections of the trajectories of the contact points tyre-road are parallel lines situated in the plane  $Q$ . In Fig. 3,  $H$  is the horizontal plane,  $O_1A$  a segment on the intersection of planes  $Q$  and  $H$ ,  $\alpha$  is the angle between  $Q$  and  $H$ ,  $n$  the unit vector defining the direction with the highest inclination of the plane  $Q$ , and  $P$  the projection of  $G$  in the plane  $Q$ , which describes the line  $O_1P$ . A mobile reference frame  $T_1$  of an orthogonal set of vectors  $i$ , is attached to  $P$  ( $i_1, i_2 \subset Q$ , the sense of  $i_1$  is along the vehicle motion direction). A fixed reference frame  $T_0$  of an orthogonal set of vectors  $k$ , is attached to  $O_1$ . The relation between  $i$  and  $k$  is given by

$$\begin{bmatrix} i_1 \\ i_2 \\ i_3 \end{bmatrix} = \begin{bmatrix} -\sin\beta & \cos\alpha\cos\beta & \sin\alpha\cos\beta \\ -\cos\beta & -\cos\alpha\sin\beta & -\sin\alpha\sin\beta \\ 0 & -\sin\alpha & \cos\alpha \end{bmatrix} \begin{bmatrix} k_1 \\ k_2 \\ k_3 \end{bmatrix}, \quad (8)$$

where  $\alpha$ ,  $0 \leq \alpha \leq \pi/2$ , and  $\beta$ ,  $-\pi \leq \beta \leq \pi$ , are the relative angular displacements of  $g$  having the directions  $i_1$  and  $i_2$ .

The roll and pinch angles are  $n = k_2 \cos\alpha + k_3 \sin\alpha$  and  $i_1 = n \cos\beta - k_1 \sin\beta$ , where  $n$  is the unit vector defining the direction with the highest inclination of the faces of tetrahedron  $Q$  with respect to  $H$ .

A new mobile frame  $T$  of base vectors  $u$  of the principal inertial directions of the sprung mass, is assigned fixed on the sprung mass (Fig. 4)

$$\begin{bmatrix} u_1 \\ u_2 \\ u_3 \end{bmatrix} = \begin{bmatrix} 1 & 0 & -\theta_2 \\ 0 & 1 & \theta \\ \theta_2 & -\theta_1 & 1 \end{bmatrix} \begin{bmatrix} i_1 \\ i_2 \\ i_3 \end{bmatrix}, \quad (9)$$

with  $i_1 \times u_1 = \tilde{\gamma} \sin \theta$ ,  $i_2 \times \tilde{\gamma} = i_1 \sin \psi$ ,  $\tilde{\gamma} \times u_2 = u_1 \sin \varphi$ , and  $\theta$ ,  $\varphi$  and  $\psi$  are the Euler angles. The frame  $T$  rotates with respect to  $T_1$  to angular velocity  $\omega$  defined as

$$\omega = \omega_1 u_1 + \omega_2 u_2 + \omega_3 u_3, \quad (10)$$

$$\omega_1 = \dot{\psi} + \dot{\varphi} = \dot{\theta}_1, \quad \omega_2 = \dot{\theta}_2, \quad \omega_3 = 0. \quad (11)$$

The motion equations of the sprung mass  $m$  with respect to  $T_0$ , with neglecting of the term  $\omega \times \tau \omega$ , are written under the form

$$m \frac{d^2}{dt^2}(OG) = R, \quad \tau_c \dot{\omega} = M_G, \quad (12)$$

where  $\tau_c$  is the moment of central principal inertia tensor,  $R$  the force acting on  $m$ ,  $M_G$  the moment with respect to  $G$ . The force  $R$  acting on the sprung mass is defined as

$$R = F + F_a + F_w + \sum_j P_j. \quad (13)$$

Here  $F = -mgk_3$  is the weight,  $F_a = F_a^1 i_1 + F_a^3 i_3$ ,  $F_a^2 = 0$  the aerodynamic force applied in the pressure center  $P_1$  linked on the frame  $T_1$ , on the position vector  $\rho_{P_1} = l_a^1 i_1 + l_a^3 i_3$ ,  $l_a^2 = 0$ , depending only on the speed  $v$  of the vehicle,

$F_w = \sum_k F_w^k i_k$  the wind force applied in the point  $P_2$  linked on the frame  $T_1$ , on the

position vector  $\rho_{P_2} = \sum_k l_w^k i_k$ , and supposed to be a constant. The quantities  $P_j$  are

the constraint forces acting in points  $A_j$ ,  $j=1,2,3,4$ , that link the sprung mass  $m$  to four unsprung masses  $m_j$ ,  $j=1,2,3,4$  of the tires  $B_j$ ,  $j=1,2,3,4$  (Fig. 5).

The variation  $\Delta V_j$  of the normal reaction forces in points  $A_j$  is given by  $\Delta V_j = -\sum_j c_j \Delta_j - \sum_j k_j \dot{\Delta}_j$ , where  $c_j$  and  $k_j$ ,  $j=1,2,3,4$ , are stiffness and damping coefficients of the suspensions associated to the static equilibrium point

$\Delta_j = 0$  of  $A_j$ . The quantities  $\Delta_j$  represent the variation of the distance between the mass centers of the tires  $B_j$  and the points  $A_j$

$$\Delta_j = z - z_j + \alpha b_j - \beta a_j, \quad j=1,2,3,4. \quad (14)$$

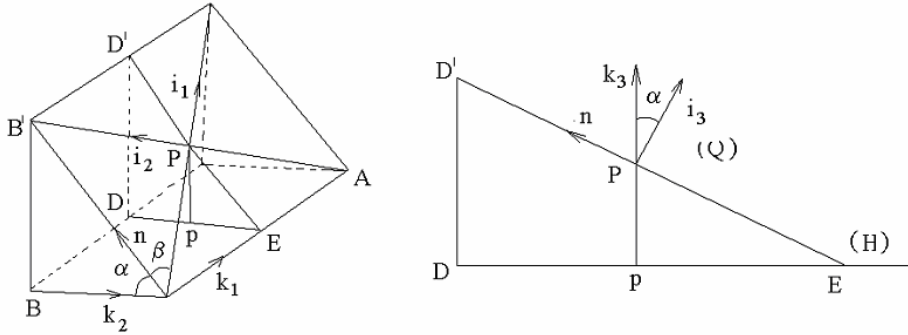


Fig. 3 – Geometry of the problem.

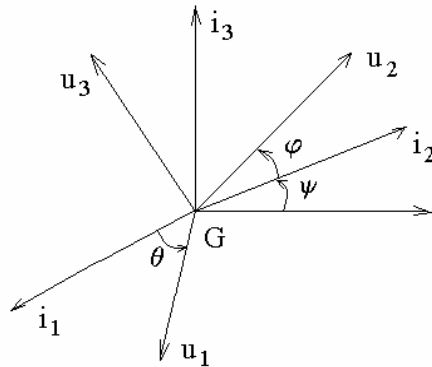


Fig. 4 – The Euler angles.

The initial conditions of the system motion are

$$t = 0, \quad v = 0, \quad F_a = 0, \quad P_j = P_j^0, \quad \varphi = \varphi_0, \quad \Psi = \Psi_0,$$

$$\theta = \theta_0, \quad \varphi_0 + \Psi_0 = \alpha_0, \quad \theta_0 = \beta_0. \quad (15)$$

From (3.6) we have at  $t = 0$

$$R_0 = F + F_w + \sum_j P_j^0 = 0. \quad (16)$$

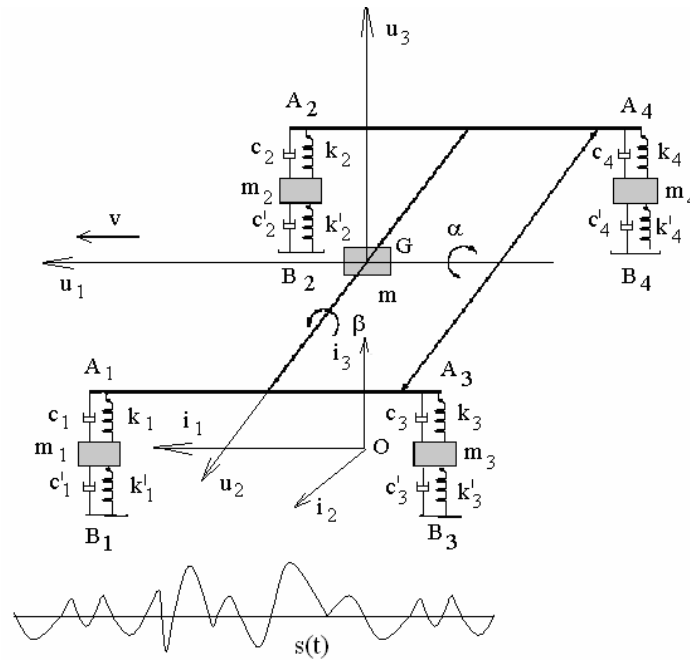


Fig. 5 – The full car model with seven degrees of freedom.

The suspension of the vehicle with two symmetric axes are modeled by the following seven equations of motion for  $m$  and  $m_j$ ,  $j=1,2,3,4$ , on the direction  $i_3$ , and the second equation (12)

$$m\ddot{z} + \sum_j c_j \dot{\Delta}_j + \sum_j k_j \Delta_j = F_a^3, \quad (17)$$

$$m_j \ddot{z}_j + c'_j \dot{z}_j + k'_j z_j - c_j \dot{\Delta}_j - k_j \Delta_j = g_j, \quad j=1,2,3,4, \quad (18)$$

$$A\ddot{\alpha} + \sum_j b_j c_j \dot{\Delta}_j + \sum_j b_j k_j \Delta_j = M_1, \quad (19)$$

$$B\ddot{\beta} - \sum_j a_j c_j \dot{\Delta}_j - \sum_j a_j k_j \Delta_j = M_2, \quad (20)$$

where  $c'_j$  and  $k'_j$ ,  $j=1,2,3,4$ , are the stiffness and damping coefficients of the tires  $B_j$ ,  $M_1$  and  $M_2$  are the moments acting on the mass  $m$  with respect to  $G$ , and  $A, B$  the principal central inertial moments corresponding to the directions  $u_1$  and  $u_2$ . The forces  $g_j$ ,  $j=1,2,3,4$ , are given by



$$g_j = c'_j s_j + k'_j \dot{s}_j, \quad j = 1, 2, 3, 4, \quad (21)$$

with  $s_j(t)$ ,  $j = 1, 2, 3, 4$ , the bristle displacement functions.

The boundary conditions attached to the tires can be written as

$$M_j = z_0 F_{ffj}, \quad F_{shj} = F_{cj} - F_z, \quad j = 1, 2, 3, 4, \quad (22)$$

where  $M_j$  are the bending moment of  $B_j$  corresponding to the contact domain,  $F_z$  is the vertical load acting on  $B_j$ , and  $F_{sh}$  is the shearing force in  $B_j$ , respectively. The moments  $M_j$  are equal to the couple moments created by the friction force  $F_{ffj}$ ,  $j = 1, 2, 3, 4$  in  $B_j$ . The friction force  $F_{ffj}$  is given by [18, 19]

$$F_{ij} = \begin{cases} k_{ffj} s_j(t_0) + \int_{t_0}^t v_{ij} dt, & |s_j| < s_{j\max}, \\ \mu \frac{|F_{cj}|}{k_{ffj}} \frac{v_{ij}}{|v_{ij}|}, & \text{otherwise,} \end{cases} \quad (23)$$

where  $k_{ffj}$  is the bristle stiffness,  $s_j(t)$  the bristle displacement functions,  $j = 1, 2, 3, 4$ ,  $t_0$  is the start time of the last sticking at that contact point,  $v_{ij}$  the relative tangential velocity in  $B_j$  and parameter  $s_{j\max}$  is the maximum allowable deflection of the bristle. The contact force  $F_{cj}$  are the contact forces in  $B_j$ , given by [17]

$$F_{cj} = k \delta^{n_j} + b \delta^{p_j} \dot{\delta}^{q_j}, \quad j = 1, 2, 3, 4, \quad (24)$$

with  $n_j, p_j, q_j$ ,  $j = 1, 2, 3, 4$ , are constants, the coefficient  $k$  depends on the tire's material and the geometric properties of the tire, and  $b$  is defined with respect to the coefficient of restitution  $0 \leq e \leq 1$ , and the  $F_{ij}$  are friction forces in  $B_j$  respectively, given by (23).

In the following we consider that the stiffness and damping coefficients  $c'_j$  and  $k'_j$ ,  $j = 1, 2, 3, 4$ , of the tires are constants. The suspension force is considered to vary continuously between a soft suspension (to insulate against road disturbances), and a hard suspension (to insulate against load disturbances)

$$c_1 = c_2 = c_1(t), \quad c_3 = c_4 = c_2(t), \quad k_1 = k_2 = k_1(t), \quad k_3 = k_4 = k_2(t). \quad (25)$$

$$c_{1,2} = \begin{cases} c_s^h, & \text{if } c_s^h < c_s \text{ (hard suspension),} \\ c_s, & \text{if } c_s^s < c_s < c_s^h, \\ c_s^s, & \text{if } c_s < c_s^s \text{ (soft suspension).} \end{cases} \quad (26)$$

$$k_{1,2} = \begin{cases} k_s^h, & \text{if } k_s^h < k_s \text{ (hard suspension),} \\ k_s, & \text{if } k_s^s < k_s < k_s^h, \\ k_s^s, & \text{if } k_s < k_s^s \text{ (soft suspension).} \end{cases} \quad (27)$$

#### 4. RESULTS

We select the following parameters for the model:  $m = 1500 \text{ kg}$ ,  $m_1 = m_2 = 40 \text{ kg}$ ,  $m_3 = m_4 = 40 \text{ kg}$ ,  $k_i' = 250 \text{ kN/m}$ ,  $c_i' = 0.6 \text{ kN/m}$ ,  $i = 1, 2, 3, 4$ ,  $k^h = 20 \text{ kN/m}$ ,  $k^s = 12 \text{ kN/m}$ ,  $c^h = 5 \text{ kNs/m}$ ,  $c^s = 0.5 \text{ kNs/m}$ . The identification of the contact patches in the interval  $T_0$  is performed by checking the minimum distance between bodies according to (1) and (2). As results, for a speed of the vehicle of  $10 \text{ m/s}$ , a number of more than 500 contact points were detected in the given interval of time in  $t \in T_0 = [0; 5\text{s}]$ . By defining a contact patch consisting from a minimum nearest 5 contact points, a number of more than 100 contact patches were identified. The functions of bristle-displacement  $s_j(t)$ ,  $j = 1, 2, 3, 4$ , are represented in Fig. 6.

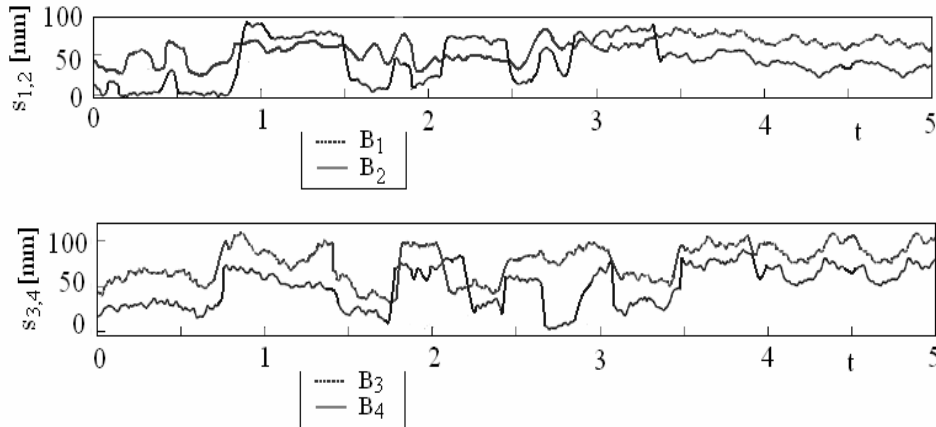


Fig. 6 – Functions of bristle-displacement  $s_j(t)$ .

Table 1 shows the characteristics of eight contact patches identified in  $T_0$  for four values of the vertical loads, 2 000, 3 000, 5 000 and 8 000 N, respectively.

*Table 1*

Dimensions of the contact patches in the interval  $T_0$

| Tire           | Vertical load<br>$F_z$ [N] | $a$ [mm] | $b$ [mm] | $n$  |
|----------------|----------------------------|----------|----------|------|
| B <sub>1</sub> | 2000                       | 35       | 46       | 2.02 |
|                |                            | 38.3     | 51.2     | 2.18 |
|                | 3000                       | 45.2     | 53.9     | 2.41 |
|                |                            | 50.2     | 54.8     | 2.55 |
|                | 5000                       | 67.8     | 63.4     | 2.88 |
|                |                            | 72.9     | 65.6     | 2.92 |
| 8000           | 90.1                       | 71.8     | 3.18     |      |
|                | 91.8                       | 74.7     | 3.95     |      |
| B <sub>2</sub> | 2000                       | 35.3     | 45.6     | 2.02 |
|                |                            | 38.1     | 51.5     | 2.17 |
|                | 3000                       | 45.0     | 53.7     | 2.40 |
|                |                            | 51.0     | 54.4     | 2.53 |
|                | 5000                       | 68.0     | 63.2     | 2.86 |
|                |                            | 73.6     | 65.5     | 2.91 |
| 8000           | 89.5                       | 72.3     | 3.15     |      |
|                | 92.5                       | 74.9     | 3.93     |      |
| B <sub>3</sub> | 2000                       | 35.8     | 45.9     | 2.03 |
|                |                            | 38.5     | 51.7     | 2.16 |
|                | 3000                       | 49.2     | 56.8     | 2.42 |
|                |                            | 61.4     | 64.5     | 2.54 |
|                | 5000                       | 52.7     | 57.0     | 2.67 |
|                |                            | 63.4     | 61.2     | 2.71 |
| 8000           | 97.8                       | 75.1     | 4.03     |      |
|                | 101.0                      | 76.4     | 4.13     |      |
| B <sub>4</sub> | 2000                       | 35.9     | 45.8     | 2.03 |
|                |                            | 38.5     | 51.8     | 2.15 |
|                | 3000                       | 53.1     | 57.1     | 2.66 |
|                |                            | 63.8     | 61.4     | 2.70 |
|                | 5000                       | 71.9     | 68.0     | 2.78 |
|                |                            | 79.2     | 67.6     | 3.00 |
| 8000           | 98.3                       | 75.0     | 4.04     |      |
|                | 100.1                      | 76.3     | 4.11     |      |

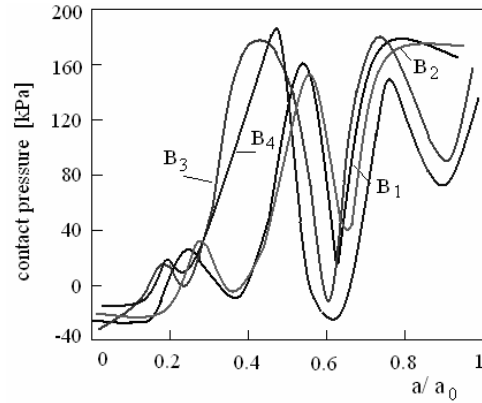


Fig. 7 – The maximum contact pressure in the first contact patch.

The maximum value of the contact pressures for the first contact patch, with respect to  $a/a_0$  and  $b/b_0$ , are plotted in Fig. 7. The  $a_0$  and  $b_0$  are the reference radii of the oval shape of the contact domain. The time variation of the roll and pinch angles  $\alpha$  and  $\beta$ , are shown in Fig. 8.

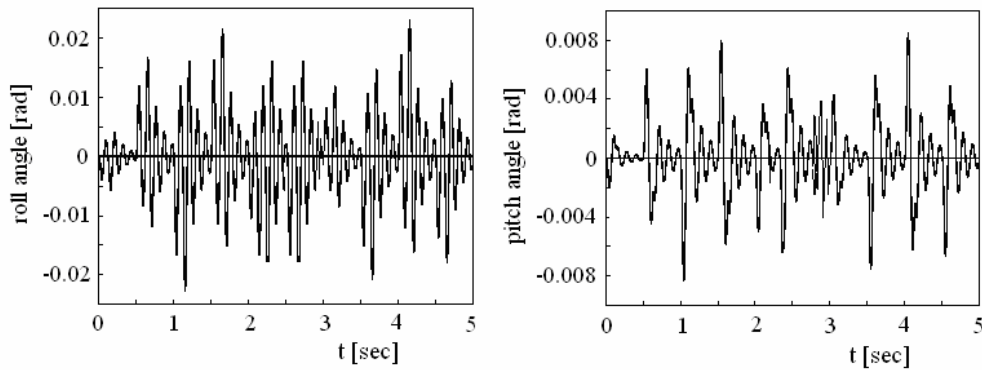


Fig. 8 – The time variation of the roll and pinch angles  $\alpha$  and  $\beta$ .

## 5. CONCLUSIONS

Road profiles are central into investigation of the interaction between the tire and the road. This paper outlines a novel approach for the modeling of the tire/road contact dynamics by assuming a full-car vehicle model in interaction with a rocky road. The vehicle model to be used in simulation is a seven degree of freedom full-car model. The response from road disturbances is analyzed by assuming an explicit relationship between the contact force and the deformation. An important

aspect of this model is that the contact area increases with deformation and a plastic region can appear for larger indentation, i.e. the damping depends on the indentation. Another advantage of this model is that the contact force has no discontinuities at initial contact and separation, and it begins and finishes with the value of zero.

For a rocky road, the bumpiness has to be taken into account. It is not unusual for automotive designers to test virtual models of cars on virtual models of bumpy roads. The bristle model for the friction force is chosen in this paper to take into account the effect of the road irregularities on the tire's action.

The suspension force is considered to vary continuously between a soft suspension (to insulate against road disturbances), and a hard suspension (to insulate against load disturbances).

The contact domain between the tire and the road has a shape defined by the Lamé curve, and it is identified by checking the minimum distance between bodies in contact.

**Acknowledgements.** This research was elaborated through the PN-II-PT-PCCA-2011-3.1-0190 Project of the National Authority for Scientific Research (ANCS, UEFISCDI), Romania. The authors acknowledge the similar and equal contributions to this article.

*Received on May 7, 2013*

#### REFERENCES

1. JALALI, H., AHMADIAN, H., POURAHMADIAN, F., *Identification of micro-vibro-impacts at boundary condition of a nonlinear beam*, Mechanical Systems and Signal Processing, **25**, 3, pp. 1073–1085, 2011.
2. FERRI, A.A., *Friction damping and isolation systems*, Journal of mechanical Design, **117**, B, pp. 196–206, 1995.
3. BERGER, E.J., *Friction modeling for dynamic system simulation*, Applied Mechanics Reviews, **55**, 6, pp. 535–577, 2002.
4. GILARDI, G., SHARF, I., *Literature survey of contact dynamics modelling*, Mechanism and Machine Theory, **37**, 10, pp. 1213–1239, 2002.
5. KARNOPP, D., *Computer simulation of stick-slip friction in mechanical dynamic systems*, Journal of Dynamic Systems, Measurement, and Control, **107**, pp. 100–103, 1985.
6. MENQ, C.H., BIELAK, J., GRIFFIN, J.H., *The influence of microslip on vibratory response, Part I: A new microslip model*, Journal of Sound and Vibration, **107**, 2, pp. 279–293, 1986.
7. BRIȘAN, C., VASIU, R.V., MUNTEANU, L., *A modular road auto-generating algorithm for developing the road models for driving simulators*, Transportation Research part C: Emerging Technologies, **26**, pp. 269–284, 2013.
8. MUNTEANU, L., BRIȘAN, C., DUMITRIU, D., VASIU, R.V., CHIROIU, V., MELINTE, O., VLĂDĂREANU, V., *On the modeling of the tire/road dynamic contact*, Transportation Research part C: Emerging Technologies, 2013.
9. DUMITRIU, D., MUNTEANU, L., BRIȘAN, C., CHIROIU, V., VASIU, R.V., MELINTE, O., VLĂDĂREANU, V., *On the continuum modeling of the tire/road dynamic contact*, CMES: Computer Modeling in Engineering and Sciences, **94**, 2, pp. 159–173, 2013.

10. MUNTEANU, L., BRIȘAN, C., CHIROIU, V., DONESCU, Șt., *A 3D model for tire/road dynamic contact*, Acta Technica Napocensis, Series: Applied Mathematics and mechanics, **55**, 3, pp. 611–614, 2012.
11. KIM, S.W., *Contact dynamics and force control of flexible multi-body systems*, PhD Thesis, Department of Mechanical Engineering, McGill University, Montreal, 1999.
12. BRENDAN, J.-Y., CHAN, B. J.-Y., *Development of an off-road capable tire model for vehicle dynamics simulations*, PhD Thesis, Virginia Polytechnic Institute and State University, 2008.
13. TRUICĂ, N., NICOLAE, V., *A mathematical model for the study of oscillations of an automobile transmission and suspension*, Symposium Mechanisms and Mechanical Transmissions, Reșița, Romania, pp. 786–804, 1976.
14. MAILAT, F., DONESCU, Șt., CHIROIU, V., MUNTEANU, L., *On the nonlinear adaptive control of semi-active suspensions*, AMSE: Advances in Modelling, Series C: Automatic control, theory and applications, **60**, 5, pp. 15–28, 2005.
15. WANG, Fu-Chen, *Design and synthesis of active and passive vehicle suspensions*, PhD Thesis, University of Cambridge, Department of Engineering, 2001.
16. DUMITRIU, D., *Car vertical dynamics 3D simulator using a 7 DOF model*, Acta Technica Napocensis, Series: Applied Mathematics and Mechanics, **55**, 3, pp. 647–650, 2012.
17. HUNT, K.H., CROSSLEY, F.R.E., *Coefficient of restitution interpreted as damping in vibroimpact*, Journal of Applied Mechanics, **42**, 2, pp. 440–445, 1975.
18. HAESSIG, D.A., FRIEDLAND, B., *On the modeling and simulation of friction*, Journal of Dynamic Systems, Measurement, and Control, **113**, 3, pp. 354–362, 1991.
19. MA, O., *Contact dynamics modeling for the simulation of the space station manipulators handling payloads*, IEEE International Conference on Robotics and Automation, Vol. 2, 1995, pp. 1252–1258.